

5 RESULTADOS E DISCUSSÕES

Os resultados e as discussões obtidos no atual trabalho serão apresentados em forma de artigos científicos, uma vez que uma das finalidades de uma tese de doutorado é tornar público os aspectos levantados durante uma pesquisa. O título de cada artigo, bem como seus status são descritos abaixo:

- a) paleoenvironmental, paleoclimatic and stratigraphic implications of the mineralogical content of the Irati Formation, Paraná Basin, Brazil. Artigo em fase revisão, a ser submetido para o Journal of South America em setembro de 2018.
- b) characterization of the Assistência Member, Irati Formation, Paraná Basin, Brazil: Organic matter and Mineralogy. Artigo publicado no periódico Journal of Sedimentary Environments em março de 2018.
- c) efeitos das intrusões ígneas no conteúdo orgânico e mineralógico da Formação Irati, Bacia do Paraná, no município de Sapopema (PR), Sul do Brasil. Artigo em fase de tradução para língua inglesa.
- d) subcapítulo de discussões integradas a respeito dos resultados encontrados nos artigos citados anteriormente.

A abreviação dos nomes dos minerais apresentados nesse trabalho segue a recomendação de Kretz (1983), o qual forneceu à comunidade geológica uma lista sistematizada de abreviaturas para minerais formadores de rochas e componentes minerais. Sua lógica e simplicidade levaram à ampla aceitação entre os autores e editores que adotaram um conjunto amplamente reconhecido de minerais e símbolos para economizar espaço em texto, tabelas e figuras.

5.1 Paleoenvironmental, paleoclimatic and stratigraphic implications of the mineralogical content of the Irati Formation, Paraná Basin, Brazil (manuscrito)

5.1.1 Abstract

The Irati Formation documents a singular moment in the evolution of the Paraná Basin, when an effective restriction of water circulation between the syncline and the Panthalassa Ocean finally established a favorable environment for the deposition of organic-rich shales. The present study presents data from X-ray diffraction (XRD), scanning electron microscopy (SEM) and energy dispersive spectroscopy (EDS) for the determination of different mineralogical components of the Irati Formation. Seeking to correlate the varying mineralogical content of the formation with the paleoenvironmental, paleoclimatic and stratigraphic conditions, total organic carbon (TOC), total sulfur (S) and insoluble residue (IR) data were also utilized. The results showed that variations in mineralogical content occurred mainly in the interval where the greatest values of TOC, S and IR are found. The authigenesis of minerals such as analcime, pyrite, gypsum and barite are closely tied to the environment where they were formed, and these minerals bear within them characteristics of paleoenvironmental conditions, such as restricted water circulation, abundant organic matter, alkalinity and pelagic sedimentation. Variations in the mineralogical content of clay minerals point to an enrichment of illite in the upper interval of the Assistência Member, thus constituting a syndepositional process. The absence of kaolinite, combined with the presence of gypsum, evidences an arid condition for this interval. The compositional change of the clay minerals in the Taquaral-Assistência interface suggest a change in the depositional systems, going from purely intracratonic and siliciclastic, to a platform depositional environment with mixed sedimentation. Furthermore, the precipitation of barite at the limit between the

Irati and Serra Alta formations bears relation to a possible discontinuity between those horizons.

Keywords: Clay minerals, Authigenic minerals, Paleoenvironment, Paleoclimate, Sequence Stratigraphy.

5.1.2 Introduction

The Irati Formation (Lower Permian) documents a singular moment in the evolution of the Paraná Basin, when an effective restriction of water circulation between the syncline and the Panthalassa Ocean eventually established a hypersaline environment in the basin. Under such conditions, carbonates and evaporites accumulated in the northern portion of the basin, and organic-rich shales in the southern portion. These shales exhibit an organic content among the highest recorded in sedimentary deposits anywhere on the planet, of approximately 23%, making them a potential generator for oil deposits in the region (MILANI *et al.* 2007).

Given these exceptional values, the Irati Formation has been the object of numerous stratigraphic, sedimentological, geochemical and paleontological studies, since the last century. However, the literature is very restricted regarding information about the mineralogical content of the rocks that make up this formation (Ramos & Formoso 1976; Rodrigues & Quadros 1976; Maynard *et al.* 1996; Dos Anjos *et al.* 2008, 2010).

In general, the combined analysis of the mineralogical and geochemical content, along with sedimentological, stratigraphic and tectonic characteristics, constitutes the classic concept of sedimentary basin analysis (KELLER, 1970). Thus, mineralogy can play an important part in the resolution of some problems, such as: definition of sedimentary facies, determination of depositional environment,

characterization of sedimentary and diagenetic processes and identification of possible source areas (ORTEGA HUERTAS *et al.* 1991).

As is the case with fossils, a mineral or an association of minerals can characterize a layer and allow regional stratigraphic correlations (MORTIMORE & POMEROL, 1987). Clay minerals, for example, are ubiquitous in different types of sediments and sedimentary rocks, from desert sands to seabottom shales. Their variation in the sedimentary record can help characterize geological environments during a certain time interval, since after they are formed they constitute an active and typical part of the environment. This relation between the nature of clay minerals and different geological environments make them an important means of studying sedimentary series and basin analysis.

Despite their important applicability in paleoenvironmental, paleoclimatic and stratigraphic studies of sedimentary successions, Rocha (1993) points to the need for the prior distinction between clay minerals of detritic origin and authigenic ones. While both play an important role in different clay mineral analyses, understanding their nature is essential in order to avoid hasty conclusions. As a rule, authigenic clay minerals furnish essential information about the depositional environment in which they were formed, while detritic clay minerals furnish wider and more complex information that encompasses the source area, alteration processes, transport and deposition.

Thus, the present study seeks to determine the mineralogical content along the entire interval of the Irati Formation, in the Sapopema region, Paraná state, in Southern Brazil, relating its constituents to paleoenvironmental and paleoclimatic parameters already consolidated in other areas of Geology, such as Sequence Stratigraphy.

5.1.3 Geological Context

The area of this study encompasses the tectono-stratigraphic context of the Paraná Basin, a vast region composed of sedimentary and magmatic rocks that extend from the southern portions of Brazil, eastern Paraguay, extreme northeast of Argentina and the northwest of Uruguay, occupying a total area of approximately 1.4 million square kilometers.

The Irati Formation lies within the Gondwana I tectonic sequence, corresponding to the basal unit of the Passa Dois Group, divided into the Taquaral (lower) and Assistência (upper) members. The Taquaral Member is comprised of clayish siltites and dark grey shales with parallel lamination (SANTOS NETO, 1993), while the Assistência Member is comprised of dark grey shales and siltites with parallel lamination, with interbedded black oil shales associated with cream-colored and dark grey carbonatic horizons (HACHIRO, 1996). According to Schneider *et al.* (1974), the lithological and paleontological characteristics of the Irati Formation indicate, for the Taquaral unit, a deposition in a marine environment of calm waters, below the level of wave action. For the Assistência unit, they indicate a shallow marine environment under basin restriction conditions (little water circulation and oxygenation), which allowed the deposition of black shales and limestones that developed in platform areas, and the formation of calcium sulphate (Figure 16).

Figure 16 - Simplified chronostratigraphic scheme of the interval studied in the Paraná Basin, Irati Formation.

Age	Lithostratigraphy		Depositional setting
Permian (Artinskian)	Irati Formation (Base of the <i>Passa Dois Group</i>)	Assistência Member	Oil shale interbedded with carbonatic rocks deposited in a mixed platform setting
		Taquaral Member	Gray to black siltites and argillites deposited in an epicontinental environment with restricted water circulation

Fonte: Adapted from Milani *et al.*, 2007.

5.1.4 Methodology

In the present work, the Irati Formation was studied based on core samples of well SP-32-PR (7368384N/548618E), located in the municipality of Sapopema, northeast Paraná state, drilled by Serviço Geológico do Brasil (CPRM) in the 1970s. The analyses were carried out utilizing X-ray diffraction (XRD), scanning electron microscopy (SEM), energy dispersive spectroscopy (EDS), total organic carbon (TOC), total sulfur (S) and insoluble residue (IR).

5.1.4.1 X-ray diffraction (XRD)

All the preparation procedures for the samples and XRD analyses were carried out in the Laboratório Multiusuário de Caracterização Tecnológica (LMCT) of the Centro de Tecnologia Mineral (CETEM). The XRD method was applied to 18 samples from different depths, encompassing the Taquaral and Assistência members. Considering the interplanar distances (d) relative to the diffractometric reflections, different mineral species were identified in the $< 63 \mu\text{m}$ and $< 2 \mu\text{m}$ fractions. Utilizing the powder method, the XRD analyses were carried out in a Bruker-AXS D8 Advance Eco equipment, with $\text{Cu K}\alpha$ (40 kV/25 mA) radiation.

Randomly oriented samples of whole rock powders were prepared by filling front-loading XRD mounts (MOORE & REYNOLDS, 1997). The samples were scanned at a rate of $1^\circ 2\theta/\text{min}$ from 5° to $70^\circ 2\theta$. For the analysis of the oriented samples ($< 2 \mu\text{m}$), non-clay minerals were removed through standard chemical treatment, based on Stokes' Law (MOORE & REYNOLDS, 1997). Thus the $< 2 \mu\text{m}$ fraction were prepared by air drying a small amount of dispersed suspension on a glass slide. To help identify the clay minerals, ethylene glycol-solvated (12h) samples

and samples heated at 510°C for 1h were also prepared using well known methods (Moore and Reynolds 1997). These samples were scanned from 4° to 30° 2 θ . The qualitative interpretation of the spectrum was made by comparing results patterns from the PDF 4+ (ICDD 2014) relational database in Bruker Diffrac. EVA software.

The samples were subjected to a semi-qualitative analysis based on the identification of all crystalline phases. This analysis was carried out considering the relative height of the diffractometric peaks and the values of I/I_{cor}, which are read when importing information from the database of the Diffrac.EVA software.

5.1.4.2 Scanning electron microscopy (SEM)

The preparation of the samples for SEM analysis followed the protocol established by Laboratório de Análise Mineralógica of CENPES/Petrobras. The samples were initially fragmented, in order to offer a fresh and irregular surface, then were adhered to a brass conducting support and covered by a thin gold-palladium sheet, by the EMITECH K750X metallizer, in order to turn them into electrical conductors. The samples were then mounted on an aluminum support and analyzed in the ZEISS EVO LS-15 SEM apparatus, as backscattered electron images, operating in a high vacuum at 20 kV and working distance of 12,5 mm.

5.1.4.3 Energy dispersive spectroscopy (EDS)

The compositional maps and the EDS microanalyses were obtained with the OXFORD Inca-Aztec Microanalysis System, attached to the SEM, which furnished the compositional tables (semiquantitative) of the chemical elements identified in the form of oxides (calculated stoichiometrically). The EDS detector does not detect the elements H, He, Li and Be. The elements B, C, N and O are detectable by EDS, however, not quantified.

5.1.4.4 Total organic carbon (TOC), total sulfur (S) and insoluble residue (IR)

TOC, S and IR analyses were carried out for the entire interval of the Irati Formation. The main objective of these analyses was to correlate these parameters with the mineralogical variation of the Irati Formation. The samples analyzed were taken, on average, at every 30 cm, starting at a depth of 141,5 m, down to 180,8 m.

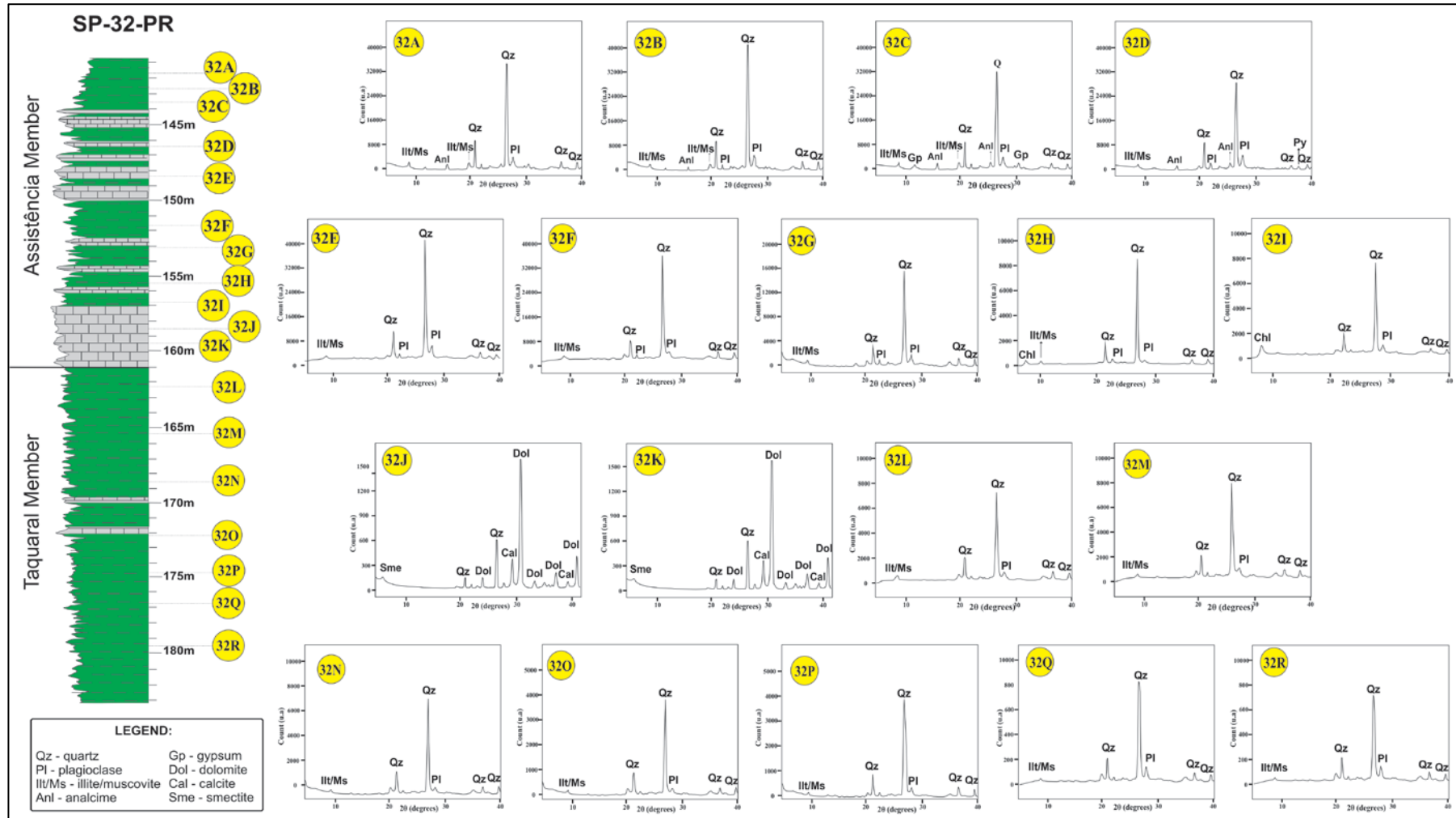
The TOC, S and IR values were obtained after the removal of the carbonatic constituents of the rocks, through a hydrochloric acid (50%) treatment. Then, they were read with a Leco SC-632 equipment. These values were registered according to the depth of each sample, allowing a semiquantitative assessment of those parameters at the different intervals analyzed.

5.1.5 Results

The diffractometric reflections, observed with XRD, allowed the characterization of the following mineral components for the pelitic portion of the Irati Formation: quartz, plagioclase, mica/illite, pyrite, analcime and gypsite (Figure 17). Based on this figure, the same mineral assemblage can be observed throughout Taquaral Member, represented by quartz, plagioclase, mica/illite and clay minerals. In the diffractograms from the Assistência Member, the diffractometric reflections indicate, besides the above minerals, the occurrence of pyrite, analcime and gypsite, preferentially in the upper interval. In the carbonatic portion, located at the base of the Assistência Member, the main diffractometric peaks are related to dolomite, calcite and quartz.

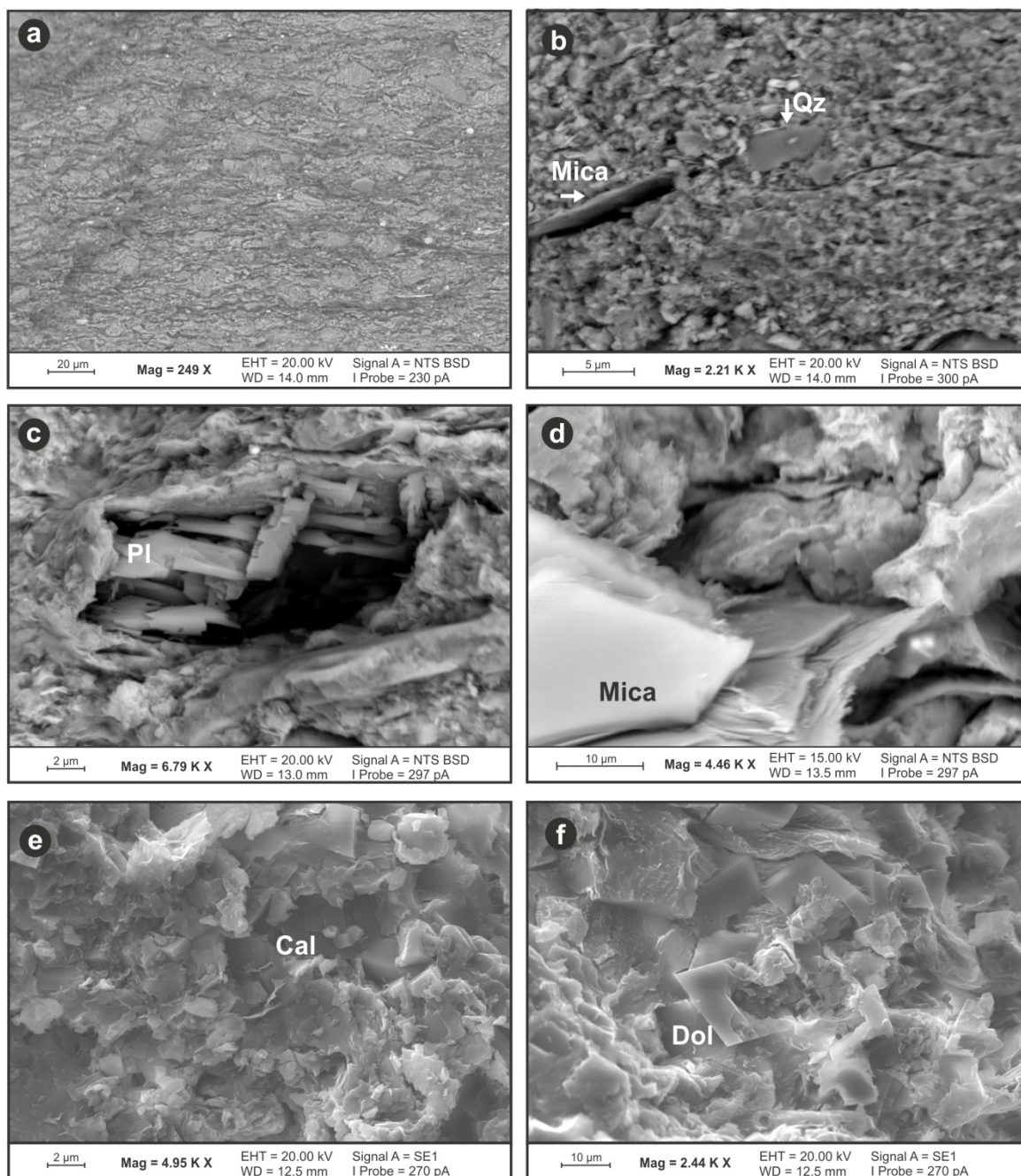
Based on the SEM analyses, it was possible to observe the fine granulometric nature of the intervals analyzed, predominantly smaller than 20 μm . The occurrence of anhedral/subhedral quartz crystals, apparently detritic, is relatively common, as well as that of partially dissolved albite crystals, silicates rich in micaceous aluminum, and euhedral carbonate crystals (dolomite and calcite) (Figure 18). In the upper interval of the Assistência Member, it was possible to observe a major concentration of framboidal pyrite, besides spheroidal analcime and gypsite filling fractures levels (Figure 19), as suggested by DRX data and ratified by EDS (Table 9). Besides these, minerals imperceptible in DRX, such as zircon and ilmenite of detritic origin, and authigenic apatite and barite disseminated in the rock matrix (Figure 20), could also be observed, through chemical composition analysis by EDS (Table 10).

Figure 17 - XRD pattern of the whole rock for samples from well SP-32-PR.



Fonte: O autor, 2018.

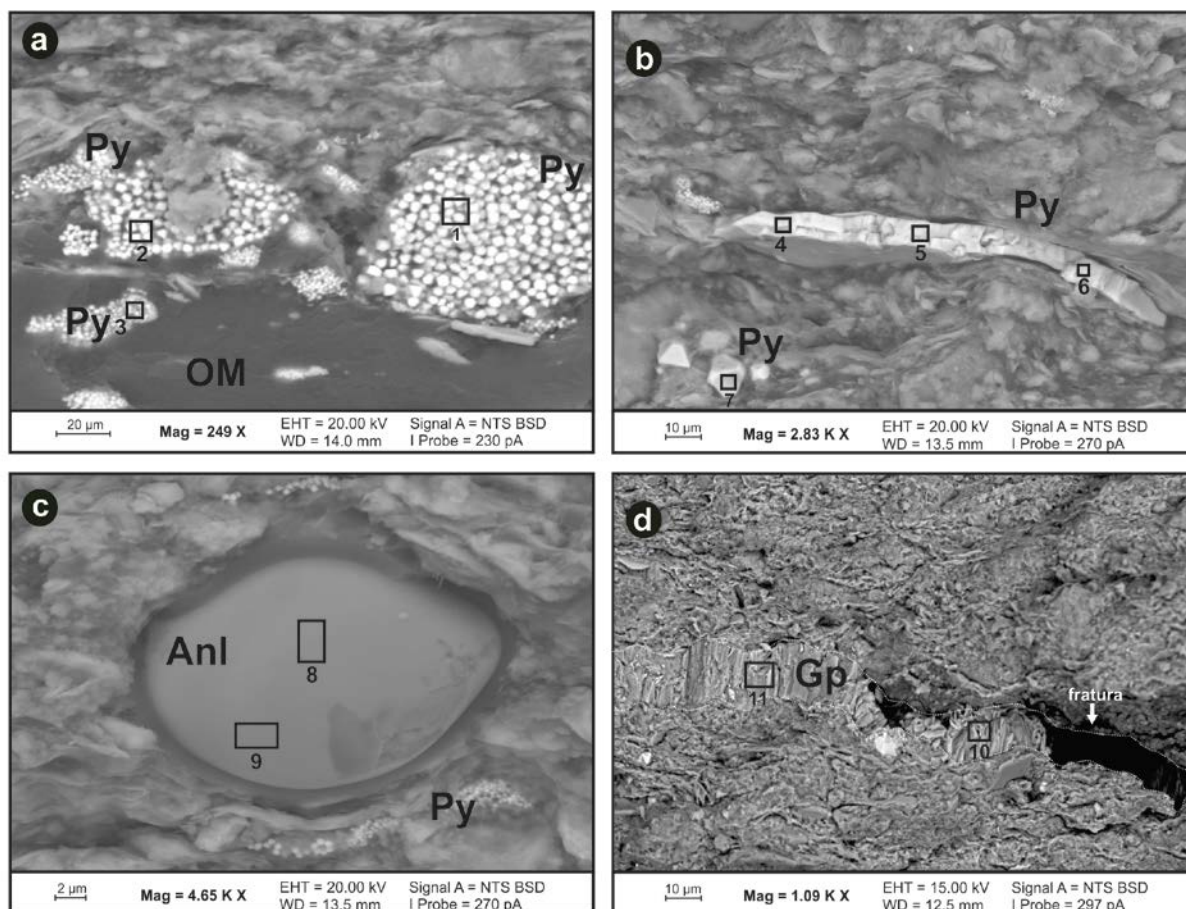
Figure 18 - SEM images of the Irati Formation in well SP-32-PR



Legend: (a) a general view of the shale, (b) presence of subhedral quartz (Qz) and mica, (c) partially dissolved plagioclase crystals (Pl), (d) detail of the micaceous habit of the aluminosilicates, (e) calcite crystals (Cal), and (f) dolomite (Dol).

Fonte: O autor, 2018.

Figure 19 - SEM images of the Irati Formation in well SP-32-PR, at a depth of 143,3m.



Legend: (a) occurrence of framboidal euhedral pyrites (Py) next to organic matter (OM), (b) pyrite crystals filling rock spaces, (c) spheroidal analcime (Anl), and (d) fracture filled by gypsum crystals (Gp).

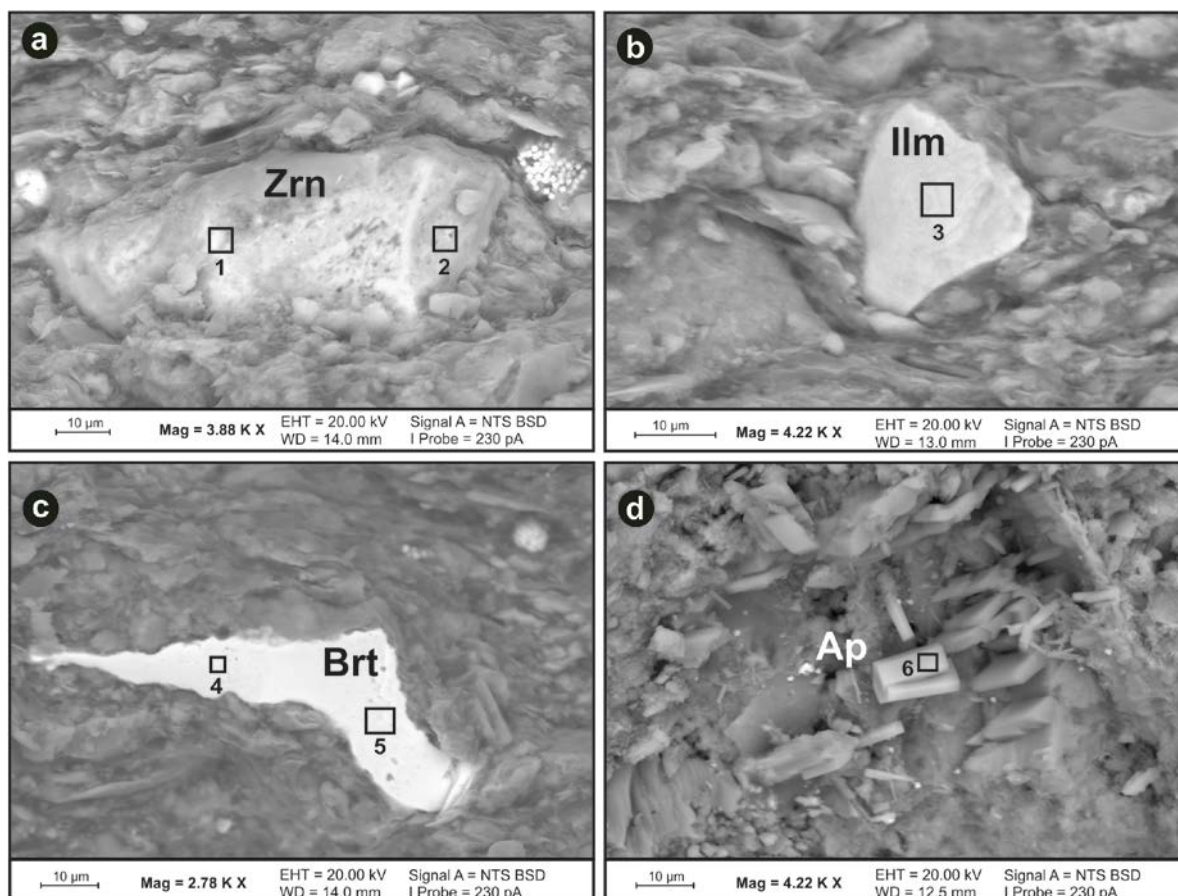
Fonte: O autor, 2018.

Table 9 - Chemical composition, in oxides, of the polygons in Figure 19.

Polygons	Na ₂ O	Al ₂ O ₃	SiO ₂	SO ₃	CaO	FeO	Total
1		0.24	0.59	55.52		43.65	100
2		0.4	0.75	69.41		29.44	100
3				68.64		31.36	100
4			1.41	68.91		29.68	100
5		0.96	2.95	54.49		41.6	100
6			2.62	66.51		30.87	100
7		1.77	6.59	58.65		32.99	100
8	12.99	22.27	64.74				100
9	12.13	22.48	65.39				100
10	1.46	1.05	3.62	56.56	37.31		100
11	0.9	0.5	1.79	57.53	39.28		100

Fonte: O autor, 2018.

Figure 20 - SEM images of the Irati Formation in well SP-32-PR.



Legend: (a) zircon crystal (Zrn), (b) ilmenite (Ilm), (c) barite (Brt), and (d) apatite (Ap).

Fonte: O autor, 2018.

Table 10 - Chemical composition, in oxides, of the polygons in Figure 20.

Polygons	F(*)	Na ₂ O	Al ₂ O ₃	SiO ₂	P ₂ O ₅	SO ₃	BaO	CaO	TiO ₂	FeO	ZrO ₂	Total
1		0.51	1.67	32.16						2.07	63.59	100
2		0.51	2.11	33.2				0.3		1.78	62.1	100
3				2.61					64.62	32.77		100
4			0.87	2.45		33.53	63.15					100
5				2.05		31.94	66.01					100
6	3.34	2.99	1.45	5.18	31.15	6.42		49.47				100

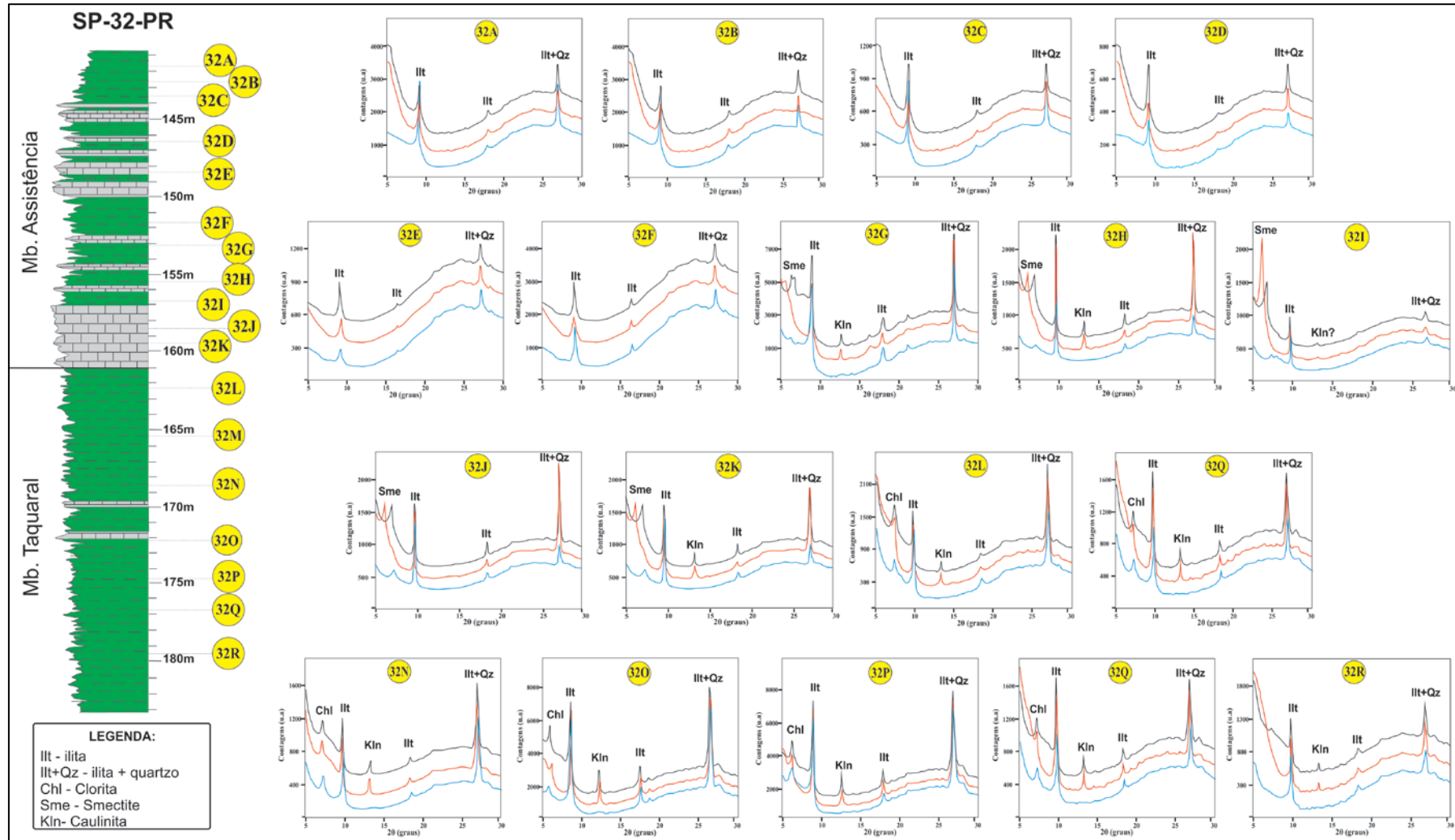
Note: Percentage in weight of the element.

Fonte: O autor, 2018.

For the $< 2 \mu\text{m}$ fraction, the diffractometric reflections indicate the occurrence of illite, chlorite, smectite and kaolinite for the Irati Formation. The Taquaral Member exhibits an assemblage of clay minerals characterized by illite, chlorite and kaolinite. The data from the Assistência Member indicates the presence of smectite, illite and kaolinite (Figure 21).

The characterization of clay minerals based on SEM images and confirmed by EDS, point to the predominance of illite and occasionally a few concentrations of chlorite in the pelitic interval. In general, the levels where clay minerals occur in a concentrated fashion confer an incipient parallel lamination to the rock. The illite occurs with a predominantly fibrous aspect, sometimes filiform, repeatedly occurring on the surface of another mineral. The aggregated chlorite crystals were observed in Rosetta shape (Figure 22). In the carbonatic interval at the base of the Assistência Member, it was possible to observe the growth of clay minerals over calcite crystals. The chemical analysis (Table 11) of these clay minerals showed high values of magnesium oxide (average of 25,84%), consistent with saponite (Figure 23).

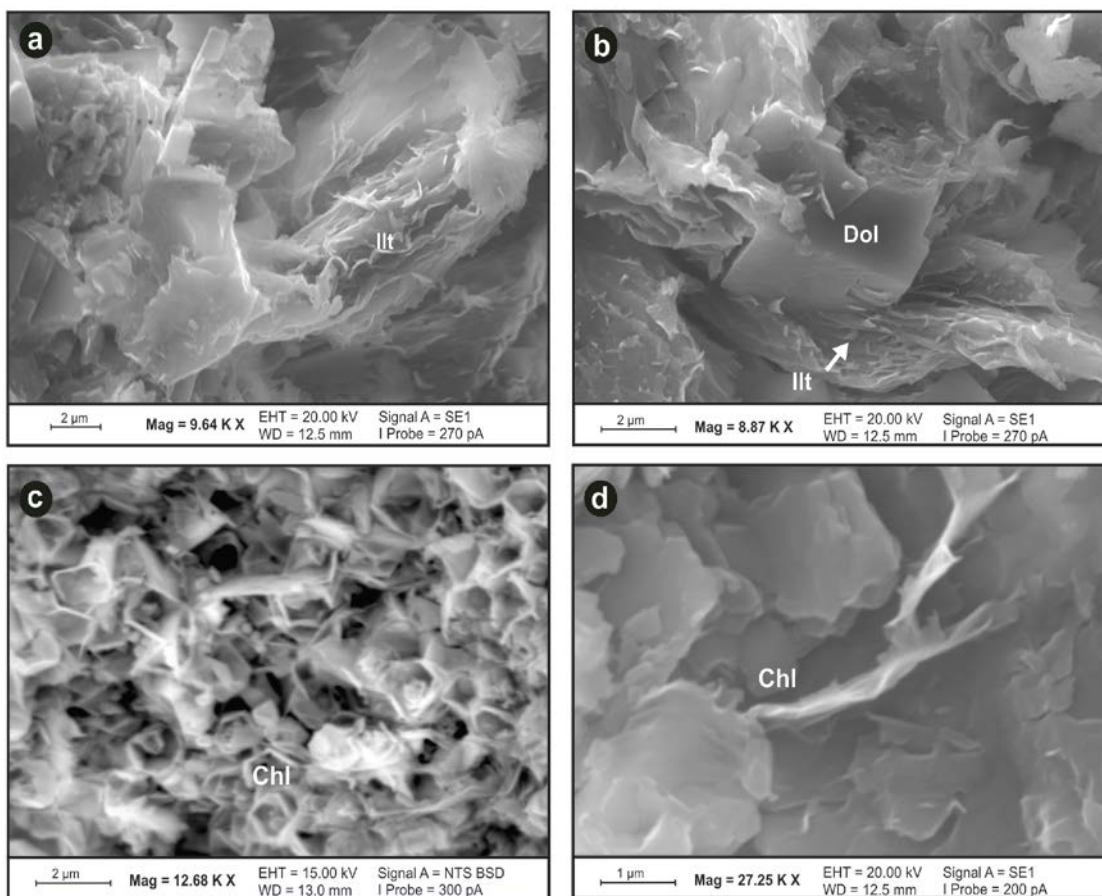
Figure 21 - XRD of the < 2 μm fraction of the samples from well SP-32-PR.



Notes: Black line – sample without treatment, red line – glycolated sample, blue line – heated sample.

Fonte: O autor, 2018.

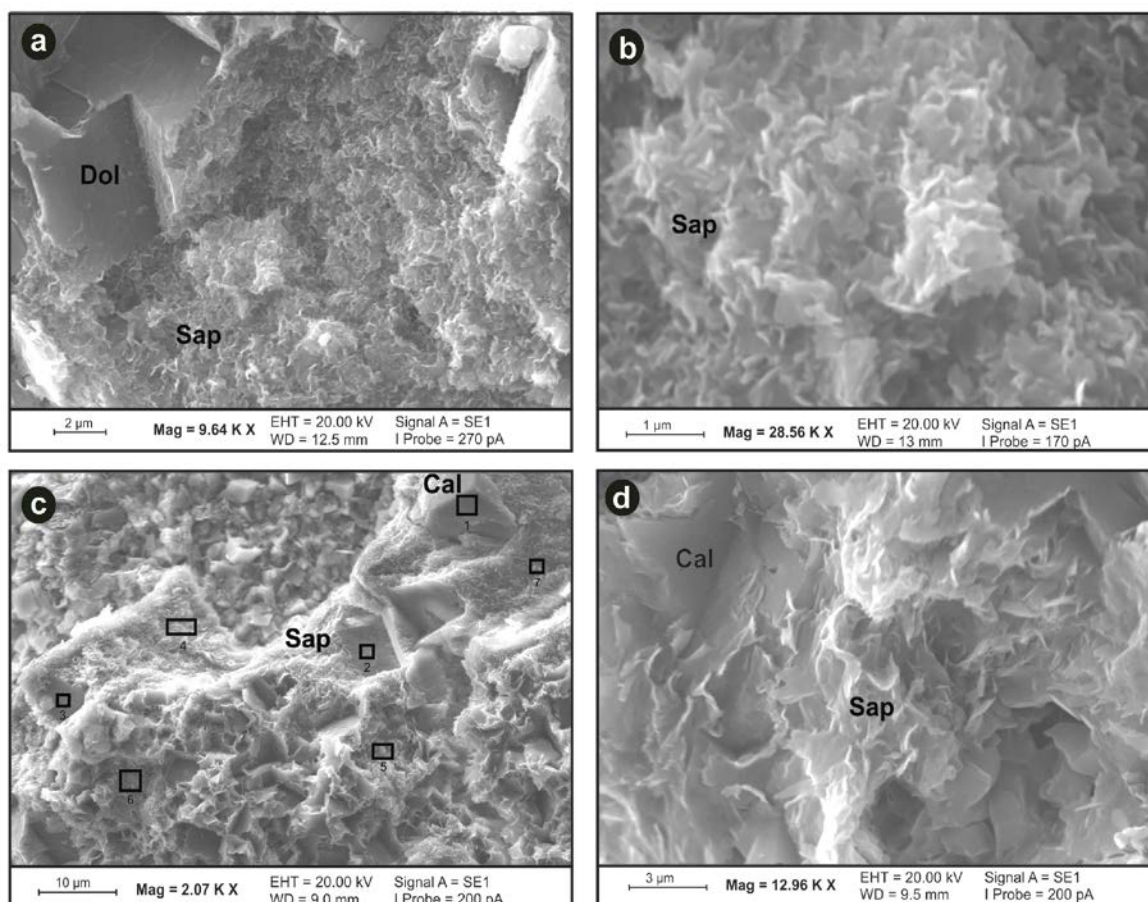
Figure 22 - SEM images of the Irati Formation in well SP-32-PR.



Legend: (a) fibrous illite crystals (Illt), (b) illite aggregates (Illt) over dolomite crystals, (c) rosetta habit of chlorite aggregates (Chl), and (d) micaceous habit of chlorite crystals (Chl).

Fonte: O autor, 2018.

Figure 23 - SEM images of the Irati Formation in well SP-32-PR.



Legend: (a) saponite aggregates (Sap) in contact with dolomite crystals (Dol), (b) saponite (Sap) in detail, and (c) saponite aggregates (Sap) over calcite grains.

Fonte: O autor, 2018.

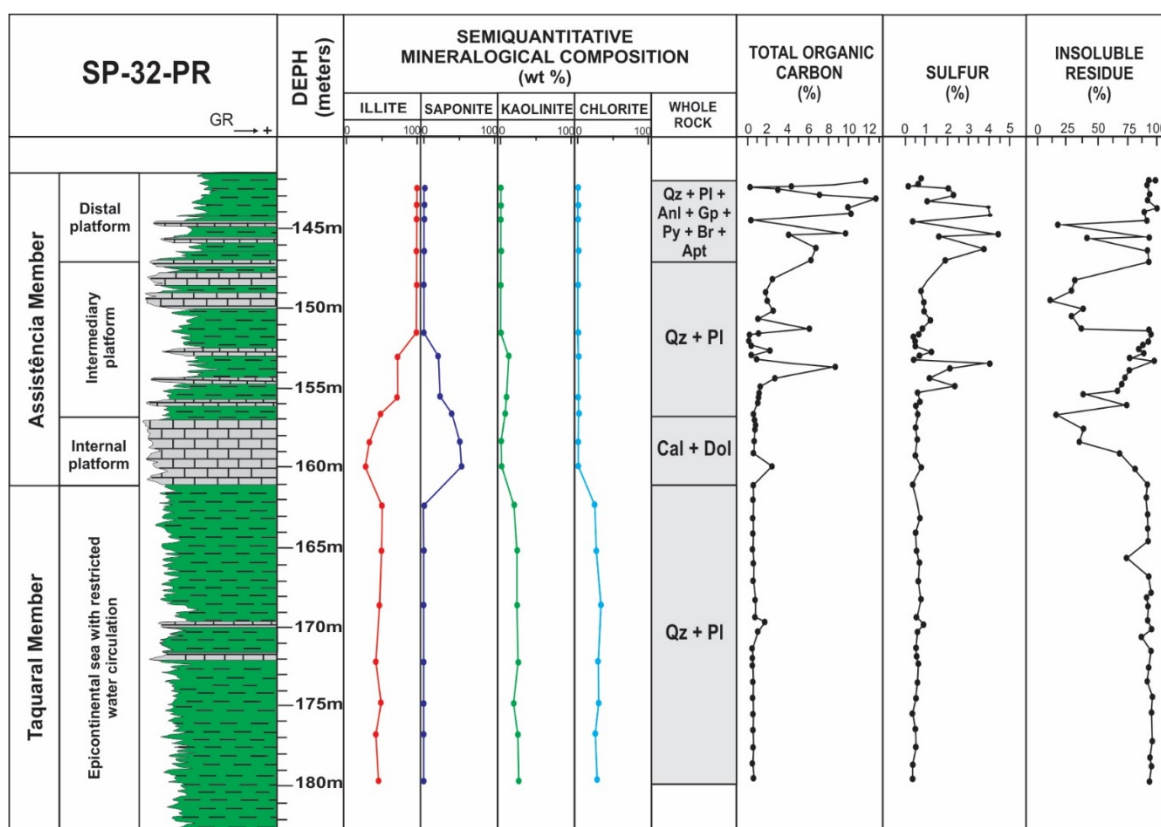
Table 11 - Chemical composition, in oxides, of the polygons in Figure 23.

Polygons	Na ₂ O	MgO	Al ₂ O ₃	SiO ₂	CaO	FeO	Total
1		1,52		1,88	96,6		100
2		3,3	0,76	3,31	92,63		100
3		5,89	1,18	7,51	85,42		100
4	2,1	24,09	5,03	60,39	2,22	6,17	100
5	2,74	29,45	6,45	58,56	0,33	2,47	100
6	2,21	25,74	3,8	46,45	8,88	12,92	100
7	2,23	24,11	4,46	51,51	4,21	13,48	100

Fonte: O autor, 2018.

When correlating TOC, S and IR information with the variation of the mineralogical content along Irati Formation, a close relation can be observed between the higher TOC and S values and the occurrence of the minerals analcime, gypsum and pyrite. Furthermore, exactly in this interval (top of the Assistência Member) diffractometric reflections that indicate kaolinite, chlorite and smectite cease occurring, while the predominant clay mineral is illite (Figure 24).

Figure 24 - Correlation between the assemblage of minerals and TOC, S and IR data for the Irati Formation, well SP-32-PR.



Notes: Qz – quartz, Pl – plagioclase, Anl – analcime, Gp – gypsum, Py – pyrite, Brt – barite.
Fonte: O autor, 2018.

5.1.6 Discussion

5.1.6.1 Minerals as indicators of paleoenvironmental conditions

According to Araújo (2001), the Irati Formation was deposited in the context of a restricted circulation between the syncline and the Paleo-Ocean Panthalassa. That restriction would have been much more effective during the deposition of the Assistência Member, creating regions where freshwater predominated (favorable for the preservation of fossils of the *Botryococcus* species) and areas where hypersaline conditions prevailed. In relation to the sedimentary paleoenvironments, the increase in TOC is directly related to ever more restricted conditions of the basin, which means a greater uniformity of physicochemical conditions of the sedimentary environment. Some significant mineralogical variations interpreted in this study occurred exactly in that interval, such as, for example, the occurrence of the minerals analcime, gypsum, pyrite and barite (Figure 24).

The occurrence of analcime is described in the literature as being relatively common in restricted alkaline environments, such as ephemeral lakes (MATTER & TRUCKER, 1978). The occurrence of analcime in a specific interval of time was interpreted by several authors (Surdam & Parker, 1972; Stoffers & Holdship 1975; Surdam & Eugster 1976; Surdam & Sheppard 1978) as being indicative of cyclic changes in salinity and alkalinity of the water of paleolakes, induced by climatic changes. According to Yuretich (1988), in this type of environment, the more restricted the water circulation, the greater the alkalinity of the depositional environment and the probability of precipitation of minerals of the zeolite group, such as analcime, shown in Figure 19(c).

The precipitation of framboidal euhedral pyrite (Figure 19(a,b)) probably occurred during the eodiagenesis stage, due to the reduction of sulfate by anaerobic bacteria. According to several studies (Berner 1968,1984; Brock *et al.* 2006; Bernard

et al. 2010), reactions of this type may be responsible for the generation of hydrogen sulphide and regions of high alkalinity. According to Berner (1984), the main controlling factor for the quantity of pyrite in a sedimentary environment is the quantity of decomposing organic matter. In Figure 19(a) it is possible to observe the occurrence of pyrite and organic matter, exactly in the interval where the highest values of TOC, S and IR occur.

The occurrence of gypsite (Figure 19(d)) follows from the context of a restricted paleoenvironment, since its formation is related to the chemical precipitation in saline environments with little water circulation (Droste, 1961; Hardier *et al.* 1968; Warren, 1999). Rosell *et al.* (1998) consider that modern environments with brackish water are sites for very high biological productivity and can be used as models for sedimentation related to evaporites. Thus, the occurrence of gypsite is associated with the interval with the highest levels of TOC and is consistent with paleoenvironmental conditions.

Apatite crystals (Figure 20(d)) may be explained based on the close relation between phosphorus and the organic material, since phosphorus is an essential chemical element of living organic matter and an important constituent of many rigid parts of animals (RUTTENBERG & BERNER, 1993). The fact that the Irati Formation has a significant fossiliferous content suggests that as the origin of the phosphorus responsible for the formation of the apatite, along with the calcium cations found in seawater. Gulbrandsen (1969) associated the precipitation of apatite crystals with restricted, saline and potentially alkaline environments.

The SEM/EDS analyses allowed the characterization of septarian barite nodules (Figure 20(c)), precisely associated with the intervals with higher organic matter concentrations. In sedimentary successions, the occurrence of barite is generally associated with sedimentation during the eodiagenetic stage, and its precipitation is closely related to pelagic sediments deposited under reducing conditions or with hiatus in the sedimentation rate (BRUMSACK, 1986; BRÉHÉRET & BRUMSACK, 2000; DICKENS, 2001; SNYDER *et al.* 2007; LASH, 2015). Its diagenetic origin is related to the migration of interstitial water rich in barium, present in rock pores, towards a zone of sulphate reduction located at the water-sediment interface.

5.1.6.2 Paleoenvironmental aspects related to clay minerals

Regarding the distribution of clay minerals in the paleodepositional context of the Irati Formation, DRX analyses (Figure 21) allowed the identification of illite in the entire interval analyzed. However, it is noteworthy that this clay mineral occurs in a concentrated fashion exactly in the upper interval of the formation, where the highest values of TOC are found. The absence of chlorite in this interval could only be due to pre- or syndepositional processes, since normal diagenetic reactions favor the preservation of this mineral, as suggested by Alves & Rodrigues (1985). The preservation of organic matter is only possible under anoxic conditions, maintained by the activity of anaerobic bacteria. These bacteria utilize the little oxygen available as well as the nitrates and sulphates of seawater to decompose part of the organic matter deposited, and release CO₂, N₂ and H₂S. The highly reducing environment thus created does not favor the preservation of chlorites, especially ferriferous chlorites, since it promotes the mobilization of the iron contained in them (LOVE, 1967; GROSSMAN *et al.* 1979). As a consequence of the mobilization of the iron contained in chlorites, the authigenesis of pyrite (FeS₂) follows, since in such an interval it is possible to observe a significant increase in sulfur content, besides small diffractometric reflections relative to the occurrence of this mineral.

Despite diffractometric reflections characteristic of kaolinite occurring throughout the Taquaral and Assistência Members (Figure 21), it was not possible to observe them in SEM/EDS analyses. However, the distribution of its occurrence based on DRX analyses suggests a relation inversely proportional to the TOC content and to the increasingly restricted aspect of basin. Araújo (2001) presented a faciological framework of the Irati Formation, and inferred three different depositional domains, characterized by an internal ramp (carbonates of the base of the Assistência Member), intermediary ramp (mixed carbonatic-siliciclastic sedimentation in the intermediary portion of the Assistência Member), and a distal ramp (carbonatic shales in the upper part of the Assistência Member). According to DRX, the absence of kaolinite in the Assistência Member is restricted to the distal platform, marked by a

high TOC content. According to Parham (1969), the kaolinite content is statistically smaller in the distal facies of sedimentary systems, as also observed in this work.

The illite concentration in the upper part of the Assistência Member may have had as a precursor mechanism either chlorite or kaolinite. Singer & Stoffers (1980), studying the vertical variation of clay minerals in lakes Albert and Manyara, in East Africa, suggest that minerals enriched in iron, present in highly reducing environments, as proposed for the upper portion of the Assistência Member, may function as a precursor mechanism favorable for the concentration of diagenetic illite, thus characterizing a syndepositional process. As in the case of chlorite, the concentration of illite in the sedimentary record is a process that may occur due to kaolinite, as long as there is an adequate supply of potassium (K). Intervals with illite concentration in lacustrine shales of the Codó Formation (Upper Aptian) of the Grajaú Basin were interpreted as being due to detrital kaolinite (GONÇALVES *et al.* 2006), and may be correlated with results obtained for the Paraná Basin in the interval studied.

5.1.6.3 Paleoclimate aspects related to clay minerals

The Irati Formation occurs in a macrocontext of climatic changes occurring during the Paleozoic, in basins located in the southern region of South America. Several studies (Gastaldo, 1996; Isbell, 2008; Goldberg & Humayun, 2010; Limarino *et al.* 2014) suggest that the Paleozoic was a period in the history of the Earth when there was a great climatic change from global glacial conditions to conditions of extreme aridity, culminating in desertic deposits, as in the case of the Botucatu Formation (Cretaceous) in the Paraná Basin. In that context, the Irati Formation is part of the postglacial stage (Cisuralian-Guadalupian), along with the Rio Bonito, Palermo and Serra Alta formations (LIMARINO *et al.* 2014).

The sedimentological, stratigraphic and paleontological characteristics do not suggest the occurrence of climatic extremes during the deposition of the Irati Formation. On the contrary, during this interval of time, there was a hot climate, probably seasonal. Holz *et al.* (2010) suggested a cyclicity between humid and dry climates, combined with small changes in the base level, which would have promoted the formation of organic-rich shales interbedded with carbonatic layers.

The DRX data (Figure 21) present diffractometric peaks that indicate a predominance of illite, chlorite and kaolinite. The distribution of these different clay minerals is constant in the Taquaral Member. Smectite, illite and kaolinite are the main constituents in the Assistência Member. Small reflections related to the mineral kaolinite present in the carbonate intervals (sample 32I) are related to the climate in the source area and not the basin, since the clay and the rock in question have an antagonistic genesis. Singer (1984), in summarizing the aspects related to paleoclimatic interpretation, based on assemblages of clay minerals, defined kaolinite as being consistent with predominantly humid climates, since its origin is directly related to high rates of chemical weathering, given its strong stability. Thus, the perceptible absence of diffractometric reflections that indicate kaolinite, in the interval where shales rich in organic matter of the Assistência Member occur, may be considered as indicative of more arid conditions in the Irati Formation.

The existence of small diffractometric reflections that indicate the occurrence of gypsum in sample 32C (Figure 17), is another evidence of a climate with a tendency towards arid conditions in the Irati Formation. The genesis of gypsum is relatively common both in marine and continental environments, as long as climatic conditions of aridity prevail during deposition (SILVA, 2000). The restricted water circulation to which the upper interval of the Assistência Member was subjected, combined with arid conditions, provided a small increase in the brine concentration, which probably culminated in the precipitation of that sulfate.

It should be noted that despite being an efficient means of paleoclimatic interpretation, the ideal would be for the analyses of clay minerals to be associated with other types of information, such as sedimentological, paleontological and stratigraphic, so that a higher reliability of the results could be achieved. Thus, the proposition of cyclic climatic conditions between humid and dry, for the Irati

Formation, is consistent with paleontological data that indicate a predominance of pinnate *Glossopteridales*, *arborescent lycophytes*, and the scarce presence of *Gangamopteris* and *Rubidgea* (palmated) fossils in the *Glossopteridales-Brasilodendron* flora (IANNUZI & SOUZA, 2005).

5.1.6.4 Minerals in the context of Sequence Stratigraphy

The sequence stratigraphy of the Irati Formation was already studied under various aspects by various authors (Lavina, 1991; Perinotto & Gama Junior, 1992; Menezes, 1994; Hachiro, 1996; Milani, 1997; Araújo, 2001; Lages, 2004; Rohn, 2007; Holz *et al.* 2010; among others). Each model presents its peculiarities, which gives rise to different points of view regarding the origin, the limits and the positioning of the main key surfaces. Some of the subtle variations in the distribution of minerals within the Irati Formation can be associated with certain aspects of sequence stratigraphy.

Some authors, among them Holz *et al.* (2010), suggest a sequence limit at the interface of the Taquaral and Assistência members, arguing that an abrupt change occurs in the deposition systems, going from siltites and argillites of the lower member, towards limestones and organic-rich shales of the upper member. This corresponds to a change from an intracratonic siliciclastic context to a context of a mixed platformal sedimentation under anoxic conditions. The DRX data (Figure 21) show a variation of the content of clay minerals starting exactly at this interface. The Taquaral Member exhibited diffractometric reflections of illite, chlorite and kaolinite; however, the Assistência Member exhibited diffractometric reflections suggest the occurrence of smectite, illite and kaolinite. The chemical EDS analyses point to the presence of saponite in the lower interval of the Assistência Member (Figure 23), which was not observed in the Taquaral Member. The magnesium contents observed in that mineral are consistent with those indicated in the study of Dos Anjos *et al.*

(2010). That change in the mineralogical assemblage may support the identification of the sequence limit suggested by Lages (2004), Rohn (2007) and Holz *et al.* (2010).

Holz *et al.* (2010) argued that the contact between the top of the Irati Formation and the base of the Serra Alta Formation is characterized by a rise in the base level that culminated with the disappearance of oil shales, the occurrence of narrow layers of rock gaps, and small fish bones, besides the appearance of small sandy, conglomeratic levels. In that context, a transgressive lag was characterized, where a second order sequence limit was inferred by the authors, between the formations. Thus, the occurrence of barite in the upper interval of the Irati Formation can also be utilized as an important stratigraphic marker. Sedimentological and stratigraphic analyses suggest that the barite precipitation is followed by prominent discontinuities in sedimentary successions (BRÉHÉRET & BRUMSACK, 2000).

5.1.7 Conclusions

In the upper interval of the Assistência Member, marked by high values of TOC, S and IR, variations in the mineralogical content were observed, which were able to help in the interpretation of the depositional paleoenvironment. The genesis of minerals such as analcyme, pyrite, gypsum and barite is generally related to environments rich in organic matter, with restricted water circulation, alkaline, and with pelagic sedimentation.

The distribution of clay minerals in the interval studied suggests that the illite concentration, in the upper interval of the Assistência Member, is related to a syndepositional process that has chlorite or even kaolinite as its precursor mechanism. In this same time interval, marked by deposition in a distal platform, conditions were not favorable to the deposition of kaolinite, which is reflected in the absence of diffractometric reflections indicative of this clay mineral.

In the context of climate changes acting during the Paleozoic, the occurrence of diffractometric reflections indicative of gypsite, combined with the absence of the clay mineral kaolinite in the stratigraphic record, represents a specific condition of aridity in the upper interval of the Assistência Member.

Interpretations related to sequence stratigraphy were carried out based on the mineralogical content observed in horizons of the Irati Formation. At the interface between Taquaral and Assistência members, DRX and SEM/EDS analyses point to the occurrence of saponite just above the interval between the two members. Furthermore, the occurrence of barite at the top of the Irati Formation was utilized as an indication for the identification of a superimposed discontinuity.

5.1.8 Acknowledgements

The authors thank all the staff of the LMCT/CETEM, where the DRX procedures were carried out, all the technical staff of the Laboratório de Pesquisa e Desenvolvimento em Exploração e Produção (PDE) of the Gerência de Integração Rocha-Perfil-Sísmica (IRPS) of CENPES/Petrobras, where the SEM/EDS analyses were carried out, and all the staff of Laboratório de Estratigrafia Química e Geoquímica Orgânica of the State University of Rio de Janeiro (LGQM/UERJ).

5.2 Characterization of the Assistência Member, Irati Formation, Paraná Basin, Brazil: Organic Matter and Mineralogy (artigo)

5.2.1 Abstract

Currently, the Irati Formation, in Paraná Basin, Brazil, represents one of the world's largest reserves of oil shale. Among the shale-derived products stands out the fuel oil, gas, naphtha, fuel, liquefied gas, and sulfur, in addition to byproducts that can be used by the asphalt, cement, agricultural, and ceramics industries. This study describes and illustrates features of organic-rich shales of the Lower Permian Assistência Member, Irati Formation, scanning electron microscopy (SEM) was combined with energy dispersive X-Ray Spectrometry (EDS), X-Ray Diffraction (XRD), total organic carbon (TOC), total sulfur (S), insoluble residue (IR) and Rock-Eval pyrolysis to characterize the mineral composition, organic matter distribution and different types of pore at the micrometric scale. These analyses were performed on samples from well SP-32-PR located in the Sapopema township, Northeast Paraná State, in South of Brazil. The investigations demonstrated that the Assistência Member has high total organic carbon (TOC) content, generation potential (S₂) and hydrogen index (HI), but is in an immature stage. The mineralogical content of the Assistência Member presents intervals rich in quartz, plagioclase, carbonates and clay minerals. Pores distribution includes intraparticle within organic matter and interparticle pores in pyrite framboids, surrounding quartz grains and between organic matter and mineral grains.

Keywords: Organic-rich shale. X-Ray Spectrometry (EDS). X-Ray Diffraction (XRD). Organic geochemistry. Rock-Eval pyrolysis.

5.2.2 Introduction

The Irati Formation (Lower Permian of the Paraná Basin, Brazil) is one of the most studied geological formations among Brazilian sedimentary formations, due to its unique fossil-bearing occurrences and high values of organic matter recorded on shales. In the past few years, the search for alternative sources of raw materials has been concentrated on shale deposits. These rocks with high organic content often represent important source rocks for oil exploration. Unconventional oil and shale gas reshaped the future energy of the planet. It has been suggested that these reserves can cover the energy needs of humanity for at least the next 135 years (CONTI et al., 2011).

Recent exploration technology advances (horizontal drilling and hydraulic fracture) have opened vast new oil and natural gas sources in shale formations. The U.S Energy Information Administration (EIA) estimates that about 15,8 trillion cubic feet of dry natural gas was produced directly from shale in the United States in 2016. This was about 60% of total dry natural gas. Shale gas production has also been established in Canada, and initial exploration drilling has begun outside North America, most notably in Poland, Argentina, India, Australia and China (CAMP et al., 2013).

In Brazil, PETROBRAS has been operating an industrial plant to explore hydrocarbons from organic-rich shale of Irati Formation. At the beginning, the Petrosix® process was established as a pilot plant in 1991, which includes procedures for mining, crushing and thermochemical processing (pyrolysis) of the organic-rich shale. Among the shale-derived products (byproducts) are fuel oil, gas, naphtha, fuel, liquefied gas, and sulfur, which in addition can be used to manufacture asphalt, cement, agricultural, and ceramics industries. According to Maraschin & Ramos (2015), the plant processes 7800 tons/day, resulting 3870 barrels of oil, 120 tons of gas, 45 tons of liquid gas and 75 tons of sulfur.

Historically, shales were thought to perform two key functions in petroleum systems: seal for conventional reservoirs and act as a source rock for hydrocarbons.

Recently, several shale formations have also proven to be major self-sourcing hydrocarbon reservoirs (DRISKILL et al., 2013).

Because of their extremely fine grain size, shale is difficult to be observed and described using conventional optical microscope techniques. However, the high magnification capability of electron microscopy allows the study of finescale rock features. Recent advances in electron microscopy technology have resulted in improved images and analytical methods to better describe, evaluate and understand shale hydrocarbon reservoir. Scanning electron microscopy (SEM) is a standard technique for identify nanometer and micrometer scale features of shales. Shale fabric at these scales provides substantial information about the origin, sedimentary and diagenetic processes, organic matter distribution and pore networks (SLATT & O'BRIEN, 2013).

Only a few studies were performed to analyze the exploratory potential of shales in Brazil (Dyini, 2006; Ramos, 2014; Maraschin & Ramos, 2015). These studies suggested that the Irati Formation is one of the main formations of the Brazilian basins with exploratory potential for shale gas and oil. Therefore, the purpose of this study is to document the primary constituents, like organic matter distribution and pore types of the Irati Formation, in the Sapopema area, located at Northeast of Paraná State, southeast of Brazil.

5.2.3 Study Area: Geologic Settings

The study area is within the tectonic and stratigraphic context of Paraná Basin, a Paleozoic syncline composed of magmatic and sedimentary rocks with ages ranging from Ordovician to Cretaceous (ZALÁN *et al.*, 1991). According to Milani *et al.* (2007), the stratigraphic record of the basin is divided into six tectonic sequences separated by interregional unconformities: the Ivaí River (Ordovician Silurian), Paraná (Devonian), Gondwana I (Carboniferous Lower Triassic), Gondwana II (Middle to Upper Triassic), Gondwana III (Upper Jurassic-Lower Cretaceous), and Bauru (Upper Cretaceous). It covers the Brazilian meridional portions and part of Paraguay, Argentina and Uruguay, with a total area of approximately 1.4 million km² (Figure 25).

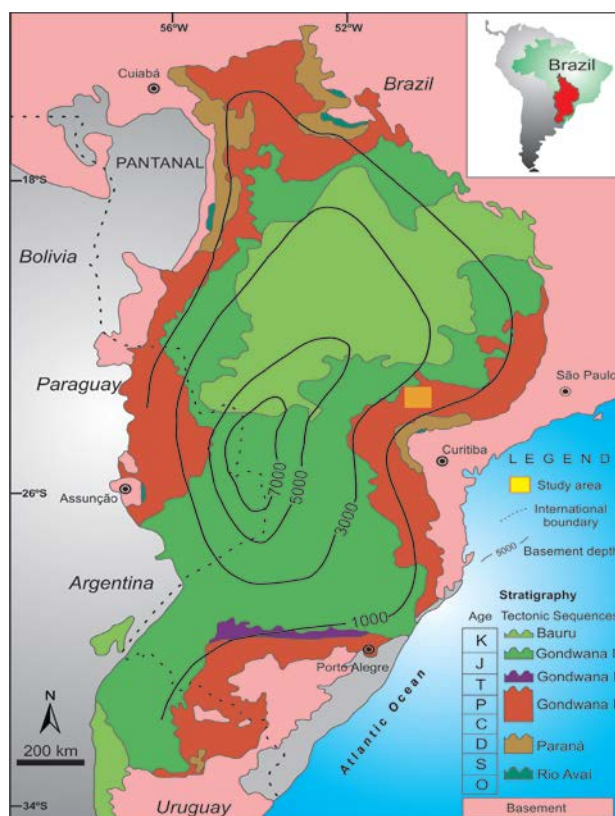
The Irati Formation was deposited during the Gondwana I tectonic sequence, in the Permian, Artinskian age (SANTOS *et al.*, 2006). It is the basal part of the Passa Dois Group and extends almost throughout the Paraná Basin. It has an average thickness of 40 m, with local peaks of about 70 m (HOLZ *et al.*, 2010); it occurs in the subsurface and is exposed in outcrops around the eastern edge of the basin.

According to Holz *et al.* (2010), the Irati Formation is divided into the lower Taquaral Member, comprising siltstones and gray mudstones, and the upper Assistência Member, formed by organic-rich shales interbedded with limestones. The Taquaral Member was deposited in a shallow marine environment (Epicontinental Sea) with restricted connection to the open ocean, and with relatively good (better) water circulation compared to the overlying Assistência Member. The depositional system of the Assistência Member includes internal, intermediary and distal ramps tilted to southwest, suggesting a possible connection to the Panthalassa Ocean only at the southernmost region of South America. Relatively deeper depositional conditions are interpreted in southern parts of the basin, which organic-rich shales predominate and total organic carbon (TOC) reaches values as high as 23% (MILANI *et al.*, 2006).

Despite the high TOC contents, the Irati Formation is thermally immature in most of the Paraná Basin. Several authors (e.g. Milani and Zalán, 1999; Araújo *et al.*, 2000; Correa & Pereira, 2005; Costa *et al.*, 2016) emphasized the role of the heat effect deriving from the diabase sills in the maturation of organic matter present in the shales. In this way, the main petroleum system of the Paraná Basin, Irati-Rio Bonito/Piramboia, is defined as a nonconventional petroleum system (MILANI *et al.*, 2006).

Based on biomarkers and isotope data, Louffi (2011) has shown a very good correlation between the oil samples recovered from Rio Bonito Formation and the organic extract from organic-rich shales of Assistência Member, of Irati Formation. Other authors (Cabral, 2006; Serafim, 2011; Vital, 2012) also found a good correlation between the oil extracted from the Piramboia oil sands and the shales of Irati Formation.

Figure 25 - Location and simplified geological map of the Paraná Basin.



Fonte: Modified from Zalán *et al.* (1991) and Costa *et al.* 2016.

5.2.4 Materials and Methods

The analyzed samples in this study belong to the SP-32PR core collected in Sapopema township, Northeast of Paraná State, southeast of Brazil (UTM coordinates 7368384N; 548618E). This region was studied in the past due to the occurrence of continuous coal layers, which led to drill news exploratory wells in the area, made by the Brazilian Geologic Survey (CPRM).

The samples were analyzed in this study area and refer to the Assistência Member from well SP-32-PR. Rock samples were cut and prepared for scanning electron microscopic (SEM) analysis. They were also analyzed by energy-dispersive X-Ray Spectrometry (EDS), X-Ray Diffraction (XRD), total organic carbon (TOC), total sulfur (S), insoluble residue (IR) and Rock-Eval pyrolysis.

5.2.4.1 Organic geochemistry data

The samples collected along the SP-32-PR core (between 141,5 m and 159,3 m) were submitted to geochemical analysis, including total organic carbon (TOC), total sulfur (S), insoluble residue (IR) and Rock- Eval pyrolysis. Geochemical analyzes were performed at the “Laboratório de Estratigrafia Química e Geoquímica Orgânica” (Chemostratigraphy and Organic Geochemistry Laboratory), of Universidade do Estado do Rio de Janeiro (LGQM/DEPA/FGEL/UERJ). The applied procedures are described in the following sub-items.

The samples were analyzed with the Leco SC-632 equipment. The first step was the elimination of carbonates using 50% hydrochloric acid. The TOC, S and IR values were plotted against the core depth. The depth plots allowed to make a semi-

quantitative assessment of organic matter concentration in the analyzed sedimentary layers.

Selected samples were analyzed with the Rock-Eval 6 equipment, of Vinci Technologies, for the determination of S_1 values (in mg HC/g rock), S_2 (in mg HC/g rock) and the temperature at which occurs the maximum peak height of S_2 (T_{max} ; °C). Considering TOC (%) concentrations, the hydrogen index was calculated [$HI = (S_2/TOC) \times 100$ in mg HC/g TOC], as well as the oxygen index [$OI = (S_3/TOC) \times 100$ in mg CO_2 /g TOC], following the procedures of Espitalié *et al.* (1985). With values of S_2 , HI and T_{max} , semiquantitative evaluations of the hydrocarbon generation potential, type and stage of thermal evolution of organic matter were carried out.

5.2.4.2 X-Ray Diffraction (XRD)

The XRD measurements were performed using a Bruker–AXS D8 Advanced Eco X-ray diffractometer, with Ni-filtered $CuK\alpha$ irradiation, at a voltage of 40 kV and a current of 25 mA, and a 2θ scanning speed of 0,01/s. Thus, step scanning from 5 to 70 and 4 to 30 2θ degrees were used for the bulk (< 63 μm) and clay mineralogy (< 2 μm) purposes, respectively. The qualitative interpretation of the spectrum was performed by comparison with standards contained in the PDF 4+ database (ICDD, 2014) in Bruker Diffrac.EVA software

To enhance the weak peaks of clay minerals, all the identified non-clay minerals were removed with both standard physical and chemical treatments (MOORE & REYNOLDS, 1997). For XRD purposes, mineralogical analyses followed the method described by Martins *et al.* (2007 and 2016). On oriented clay samples, about 3 g of fine sediment fraction of each sample were first decomposed (disaggregated by ultrasonic vibration for 1 min) and then left to stand for 20 min so that all particle sizes greater than clay-sized (< 2 μm) would settle to the bottom of the tube and leave the clay particles in suspension (according to Stoke's law), using

a 0,1% solution of $\text{Na}(\text{PO}_4)_6$ to avoid the aggregation of submicroscopic polymineralic flocculates. The suspension was removed and oriented, and dried clay preparations were made. The first slide was air-dried while the second was saturated with ethylene glycol. The third was analyzed after heating to 550°C for 1 h.

The samples were submitted to semiquantitative analysis for the identification of all crystalline phases. This analysis is performed considering the relative height of the diffractive peaks and the I/I_{cor} values, which are read importing information from the Diffrac.EVA software database.

5.2.4.3 Scanning electron microscopy (SEM) and energy-dispersive X-Ray Spectrometrie (EDS)

The preparation of samples for analysis in the SEM/EDS followed the standard established by the Laboratory of Pesquisa e Desenvolvimento em Exploração e Produção (Laboratory of Research and Development in Exploration and Production) from CENPES/PETROBRAS. Samples were initially fragmented in order to provide a fresh and irregular surface, adhered in a brass conductor and covered by a thin layer of gold-palladium, from EMITECH K750X metallizer. Then, it was adhered to aluminum conductive support and analyzed by scanning electron microscope ZEISS EVO LS-15, in backscattered electron images, operating in a high vacuum at 20 kV and with a working distance of 12,5 mm.

Composite maps and EDS microanalyses were obtained through the OXFORD Inca-AZtec Microanalyses, coupled to the SEM, which provided compositional (semiquantitative) tables of the chemical elements identified in the oxide forms.

5.2.5 Results

Table 12 presents the following information about each analyzed sample in the Assistência Member (core SP-32-PR): depth (m), lithology and organic geochemistry analyses.

The TOC content of the samples average 3,8%, ranging from 0,8 to 14,4%. The highest TOC values are associated with black shales located at the top of the Assistência Member. The S average value is about 0,96% and its higher values are associated with black shales in the top of Assistência Member. The higher IR values (> 88%) in the top of Assistência Member spread in a thickness of approximately 4,4 m, are linked with the essentially siliciclastic nature of this interval. However, bellow this depth, the Assistência Member is characterized by alternating intervals of high and low IR content, ranging from 34% to 81%. These values are associated with gray limestone interbedded by dark-gray shale.

Table 12 - Organic carbon contents and Rock-Eval pyrolysis results.

Sample n°	Depth (m)	Lithostratigraphy	Organic geochemistry							
			TOC (%)	S (%)	IR (%)	S ₁ (mg/g)	S ₂ (mg/g)	HI (mg/g)	OI (mg/g)	T _{max} (°C)
1	141,8	Black shale	5,4	0,8	88	0,9	23,8	437	9,4	426
2	142,7	Black shale	3,8	2	90	2,2	19,8	526	16,5	415
3	143,3	Black shale	14,4	0,9	94	4,5	85,6	594	8,3	422
4	146,2	Black shale	8,2	3,7	88	3,4	44,7	547,3	7,7	413
5	148,3	Dark-Gray shale	3,2	0,8	34	3	19,2	594,7	17,4	417
6	150,5	Dark-Gray shale	3,2	0,7	39	2,7	20,3	639,1	15,6	416
7	151,8	Dark-Gray shale	1,5	0,4	38	1	6,1	396,8	31,8	407
8	153,1	Dark-Gray shale	0,8	0,4	81	0	0,4	50	90,8	425
9	155,5	Dark-Gray shale	1,6	0,4	68	1,7	6,4	394,4	70,4	383
10	156,8	Dark-Gray shale	0,9	0,4	71	1,1	5,6	592,6	46,8	412
11	158,5	Gray limestone	1,1	0,3	40	0,7	4,2	377,3	35,5	402
12	159,5	Gray limestone	1,1	0,3	37	0,7	4,5	403,6	29,7	406

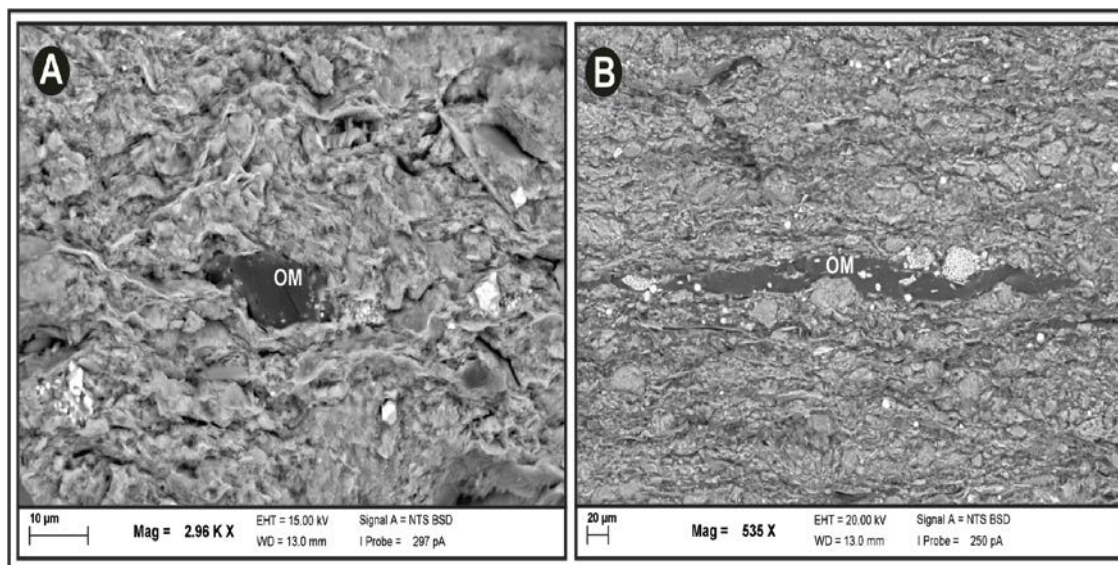
Notes: TOC = total organic carbon. S = Sulfur. S₁ and S₂ = peaks corresponding to free and kerogen-bound HC, respectively, generated by Rock-Eval pyrolysis; HI = Hydrogen index; OI = Oxygen Index; T_{max} = peak temperature of kerogen breakdown.

Fonte: O autor, 2018.

The S₁ values range from 0-4,5 mg/g. The highest value determined for this parameter corresponds to a black shale sample (143,3 m), while the lowest value was obtained in the sample of dark-grey shale (153,1 m). The S₂ values ranged from 0,4 mg/g to 85,6 mg/g, with the highest and lowest values recorded in samples of black shale (143,3 m) and dark-gray shale (153,1 m), respectively. The average value of HI was 446,7 mg/g: the highest value of this parameter was found in the black shale sample (143,3 m) and the lowest in the dark-gray limestone sample (153,1 m). In the study section, the organic material is thermally immature (T_{max} < 430 °C).

Scanning electron microscopic images showed that black shales are composed by fine-grained sediments (particles size < 20 µm), with high organic matter content. The organic matter not only coat the mineral particles but also fills most of the intergranular and grain contact regions (Figure 26).

Figure 26 - SEM images of the Assistência Member (sample 143,3 m) showing

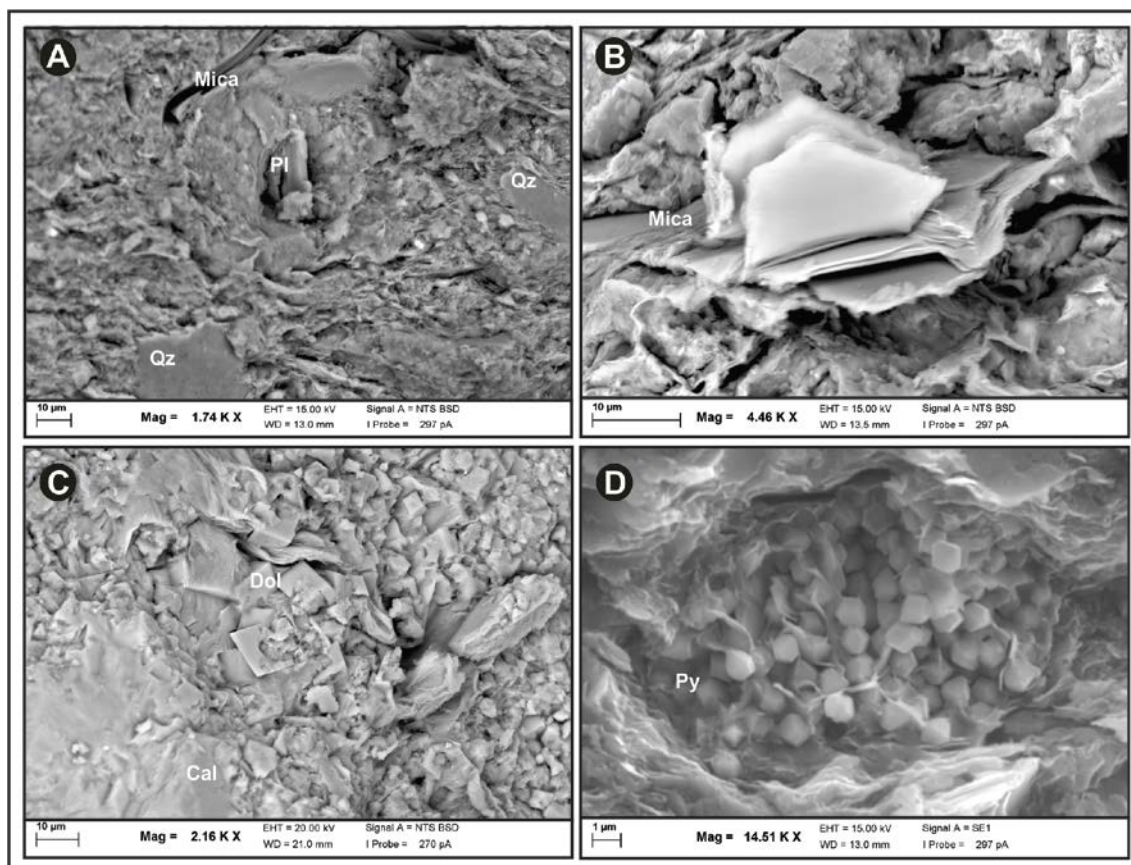


Legend: (A) Organic matter (OM) coat mineral and (B) filling of intergranular regions.

Fonte: O autor, 2018.

The black shale samples had about 36,1-40,5% of quartz and about 14-15,6% of plagioclase with small amounts of pyrite, analcime and gypsum. Among the clay minerals, there is a predominance of illite. The dark-gray shale samples showed about 29,2-37,1% of quartz and 14,8-18,4% of plagioclase. Among clay minerals occur illite, smectite and kaolinite. The gray limestones have about 33,9-36,6% of dolomite, 18-19,7% of quartz and 17,8-19% of calcite. They include illite and smectite (Table 13). SEM images indicated that a final microfabric can be influenced by the amount of silt-size particles. Examples of the most common silt-size minerals are quartz, plagioclase, carbonates (calcite and dolomite), mica and pyrite in framboids (Figure 27). Their identification was confirmed by EDS analysis.

Figure 27 - SEM images of the Assistência Member showing several types of mineral grains in a clay matrix.



Legend: (A) Sample 146,3 m: Qz = quartz. Pl = plagioclase; (B) sample 158,5 m: embedded mica sheets; (C) sample 158,5 m: carbonate (Dol = Dolomite; Cal = Calcite); (D) sample 142,5 m: framboidal pyrite (Py).

Fonte: O autor, 2018.

The clay flakes on burial could easily rotate into a parallel or sub parallel position (Figure 28). The samples from the Assistência Member had clay contents between 25,9 and 54,7% (Table 13) and were composed of illite, smectite and occasionally small amounts of kaolinite. SEM images showed that most clay minerals often formed fibrous or platelet aggregates on the surface of other minerals (Figure 29).